Mechanics of Soft Gels: Linear and Nonlinear Response

70

Mehdi Bouzid and Emanuela Del Gado

Contents

Abstract

Soft gels are materials at the core of material technological innovation, and as such, they are constantly evolving to meet different requirements in terms of performance, reliability, durability, and environmental impact. Despite many progresses made in the case of polymer gels, a consistent theoretical framework for the relationship between the microscopic structure and the mechanical properties of a wide range of materials ranging from colloidal gels to protein and biopolymer gels is still lacking. A multitude of different phenomena are

M. Bouzid (✉)
LPTMS, CNRS, Univ. Paris-Sud, Université Paris-Saclay, Orsay, France
e-mail: mehdi.bouzid@u-psud.fr; mb1853@georgetown.edu

E. Del Gado
Department of Physics, Institute for Soft Matter Synthesis and Metrology, Georgetown University, Washington, DC, USA

Kavli Institute for Theoretical Physics, University of California, Santa Barbara, CA, USA
e-mail: ed610@georgetown.edu

W. Andreoni, S. Yip (eds.), *Handbook of Materials Modeling*,
https://doi.org/10.1007/978-3-319-44680-6_129

observed – aging, strain stiffening, creep, banding, and fracture – that are difficult to control and properly tune to design the material properties. Here we discuss how numerical simulations of suitably designed microscopic models can help develop novel insight into the microscopic mechanisms that underlie the complex dynamics of these versatile materials. We provide an overview of the computational approach we have recently developed and of the main outcomes obtained. Finally we discuss outstanding questions and future developments.

1 Introduction

Gels are amorphous materials composed of a liquid phase and an interconnected network like solid phase, which can be formed at very low solid volume fractions. They are widespread, both in nature and in industry – from the pharmaceutical industry (agar gel) to the construction sector (cement hydrate or aluminosilicate gels in cement) – or in everyday life: the bread gets its rubbery texture from the formation of an elastic network of gluten protein, and the formation of protein networks is vital for the successful production of cheese. All soft matter, in fact, from proteins (Lieleg et al. 2011) to colloids (Lu et al. 2008; Gao et al. 2015) and polymers (Chen et al. 2010), easily self-assembles into such weakly elastic solids (see some examples in Fig. 1). They generally present a heterogeneous structure which is the result of the coupling between the kinetics of aggregation, phase separation or demixing, and arrest of the microscopic dynamics (Trappe et al. 2001; Del Gado et al. 2004; Coniglio et al. 2006; Del Gado and Kob 2010; Varrato et al. 2012; Zia et al. 2014).

The solidification process typically induces mechanical heterogeneities and hence internal stresses in the material, which then affect its properties in the long term (Cipelletti and Ramos 2005; Maccarrone et al. 2010a; Guo et al. 2011; Angelini et al. 2014; Bandyopadhyay et al. 2004). Weaker regions, for example, may yield via the sudden and irreversible rupture of bonds between the particles, which can be triggered by thermal fluctuations, while other regions densify. These "micro-collapses" or other aging processes can affect the stability of the material and the reliability of its performance (the mechanical strength of a gelled product can decay, for example, or batteries composed of colloidal gels may fail due to a progressive conductivity loss favored by aging (Youssry et al. 2013; Duduta et al. 2011; Helal et al. 2016; van Doorn et al. 2018)). The mechanical properties of the gel, therefore, depend on both the solidification protocol and the age of the sample. These problems are, in most of the cases, treated empirically because of the lack of fundamental understanding.

Even without the aging, it would be difficult to disentangle the impact of the structure, the dynamics, and the mechanical response in soft gels, because of the topological complexity of the solid network and of the microscopic relaxation mechanisms involved. The microscopic dynamics of gel networks is strongly cooperative and nonlocal (Colombo et al. 2013) due to the coupling among processes occurring over different lengthscales, a fact that has traditionally made theory, experimental, and computational investigations extremely challenging. Capturing

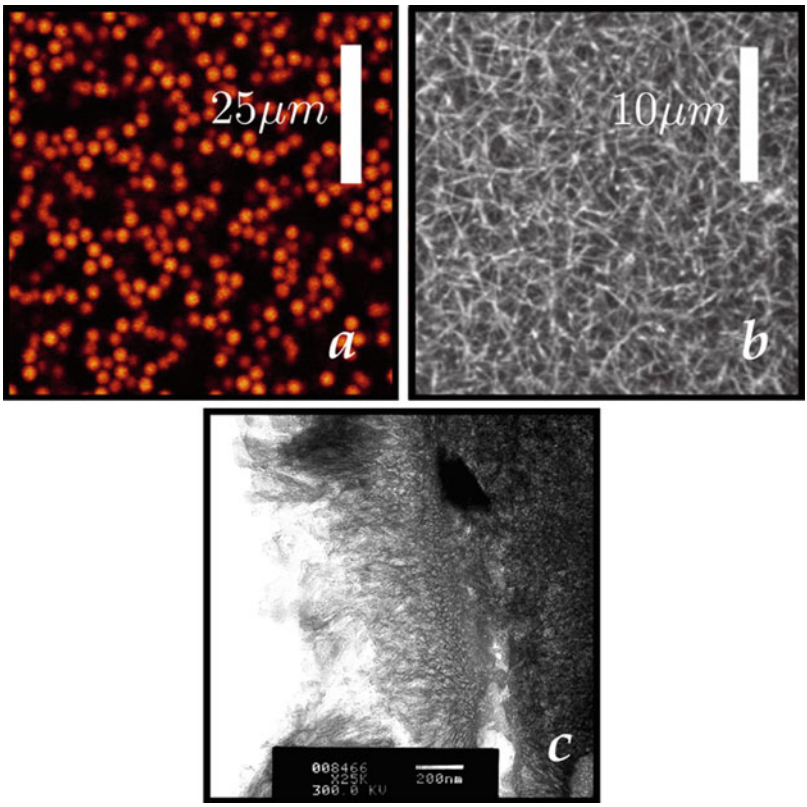

Fig. 1 (**a**) Snapshot of a colloidal particle gel (PMMA). (Reprinted from Tsurusawa et al. 2018). (**b**) A biopolymer gel (Fibrin). (Reprinted from de Cagny et al. 2016), (**c**) bright-field TEM images of calcium-silicate-hydrates C–S–H. (Reprinted from Del Gado et al. 2014)

the mechanics of soft gels and their intrinsically nonequilibrium and nonlinear nature requires bridging the lengthscale of the contacts between the particles to the lengthscale of the particles themselves and to the lengthscales relevant to the mechanics of the networks, which can include much larger structures. In addition, the presence of the fluid that can flow between the deformable pores contributes to the mechanical complexity (de Cagny et al. 2016). Under an imposed load or deformation, a multitude of different phenomena are observed – aging, strain stiffening, creep, banding, and fracture – that are difficult to rationalize, control, and properly tune to design the material properties. A key question to ask, to address this complexity, is whether or not there can be common microscopic underpinnings for the relaxation/deformation mechanisms that lead to aging at rest and to the mechanical response for different types of gel. In the last years, novel technologies have allowed experimentalists to combine rheology with imaging (Cerbino and Trappe 2008; Arevalo et al. 2015), ultrasound velocimetry (Gallot et al. 2013), interferometry (Mao et al. 2017), or spectroscopy (Ruta et al. 2012; Eberle and

Porcar 2012; Maccarrone et al. 2010b; van der Kooij et al. 2018; Aime et al. 2018b). Combining such approaches with computational studies and numerical simulations creates new unique opportunities to fill the gap between the macroscopic rheological behavior of the materials and their micro- and even nanoscale structure/dynamics and provides novel significant insights to develop advanced theories and constitutive models (Nicolas et al. 2018; Fielding 2014; Bouzid et al. 2018a).

In this chapter, we give an overview of new insights that can be gained through judiciously designed computational studies and models and of how the progress made can help understand at a more fundamental level the dynamical and mechanical complexity of soft gels. Building on the results obtained, we discuss how to tackle outstanding questions and how to bridge the microscopic picture obtained toward mesoscale or continuum level theories. The chapter is organized as follows: in Sect. 2, we present the computational approach we have recently developed for investigating the dynamics and the mechanics in a soft gel model. In particular this approach has been helpful to unravel the different nature of dynamical fluctuations in soft gels, depending on the internal stresses and the elasticity of the material, as discussed in Sect. 3. The mechanical response and its connection with the microstructure are discussed in detail in Sect. 4. Finally, in Sect. 5, we draw conclusions of the progress made so far and review some of the outstanding questions.

2 Computational Approach and Numerical Model

In the need to deepen our understanding of the interplay between the complex microstructure, the emerging dynamics, and the mechanical response of soft gels, numerical simulations play an increasingly important role. A key reason is the unique capability of computational methods to integrate different levels of complexity in a controlled manner. In condensed matter physics, the theories aimed at explaining macroscopic experimental observations are very rarely ab initio (Marx and Hutter 2009). They are based on simplified hypotheses, integrating a conceptual representation, covering a certain scale in time or space. The numerical simulations make it possible either to verify the validity of a theory by simulating the materials within the specific framework of the hypotheses used or to test the validity of the hypothesis of the theory, and to better understand their emergence, by simulating the material on a more microscopic scale. Ab initio numerical approaches are mainly useful when the microscopic details are sufficiently simple, but in most of other cases, coarse-grained approaches are more versatile and powerful. Being able to vary, in a continuous and parametrized way, the different microscopic properties is a big advantage of the numerical methods, because it makes it possible to offer a field of systematic studies out of reach of the experimental systems and, thus, to help to reveal new explanatory concepts.

Particle-based and molecular dynamics inspired approaches have proven effective, in the last few years, to unravel the dynamics and nonlinear mechanics of gel networks, thanks to large-scale simulations that can help disentangle the dynamical

processes at the level of the network structure and their contribution to the material's linear and nonlinear response (Colombo and Del Gado 2014b; Bouzid and Del Gado 2018; Bouzid et al. 2018a; Landrum et al. 2016; Jamali et al. 2017; Boromand et al. 2017; Di Michele et al. 2014; Varga and Swan 2018; Padmanabhan and Zia 2018). In these types of approaches, gels are described in terms of their microscopic discrete building blocks, typically particles, grains, or small aggregates in colloidal gels or flocculated suspensions. With a suitable model for the effective interactions between the particles, the time evolution of the system is obtained by integrating the many-body equations of motion for the whole set of microscopic degrees of freedom (typically, center of mass positions and velocities of the particles). The simulations therefore necessarily contain the following ingredients: (i) a model that describes the interactions between the particles, usually in terms of an interaction potential $\mathscr{U}(\mathbf{r}_i, \ldots, \mathbf{r}_N)$, where $\mathbf{r}_i$ represents the particle coordinates, and (ii) a numerical integrator, i.e., an algorithm that solves efficiently and precisely the equations of motion with a set of boundary conditions that corresponds to the specific problem of interest. The equations of motion can have different amount of details of the microscopic motion of the particles that compose the gel (from Brownian fluctuations to hydrodynamic interactions). With such an approach, one can introduce interactions between particles in a simple and controlled way and ask about the emergence, at various scales, of the constitutive properties of gels.

For the effective interactions, a number of approaches have been used in the literature to model soft gels, including short-range isotropic interactions typical of colloidal suspensions, valence-limited and patchy particle models that mimic small molecule or functionalized nanoparticle gels, and dipolar interactions that can lead to chaining and branching (Koumakis and Petekidis 2011; De Candia et al. 2006; Zaccarelli et al. 2006; Coniglio et al. 2004; Del Gado et al. 2004; Rovigatti and Sciortino 2011; Blaak et al. 2007; Ilg and Del Gado 2011; Eberle et al. 2011; Bianchi et al. 2015; Zia et al. 2014; Varga et al. 2015; Fierro et al. 2008). While these models mainly focus on the two-body short-range interactions that create the mechanical contact between particles at first, the emerging softness of the gel materials is the result of the sparse nature of the network structure, whose connections, on the other hand, need to be fairly rigid to support at least the gel own weight and a finite torque (Del Gado and Kob 2010, 2007; Pantina and Furst 2005, 2006; Ohtsuka et al. 2008; Colombo and Del Gado 2014a; Hsiao et al. 2012). We have therefore focused on a model where a short-range attractive well is combined with a three-body term, which imparts an angular rigidity to the gel branches, as to be expected in such open structures.

2.1 A Microscopic Model with Directional Interactions

We have developed a minimal model, considering particles (or small aggregates represented as particles) of diameter d that interact through a potential composed of two terms:

$$\mathscr{U}(\mathbf{r}_i, \ldots, \mathbf{r}_N) = \varepsilon \left[\sum_{i>j} \mathscr{U}_2 \left(\frac{\mathbf{r}_{ij}}{d} \right) + \sum_i \sum_{j>k}^{j,k\neq i} \mathscr{U}_3 \left(\frac{\mathbf{r}_{ij}}{d}, \frac{\mathbf{r}_{ik}}{d} \right) \right] \tag{1}$$

where $\mathbf{r}_{ij} = \mathbf{r}_j - \mathbf{r}_i$, with $\mathbf{r}_i$ denoting the position vector of the i-th particle and ε the strength of the attraction that sets the energy scale. The first contribution to $\mathscr{U}$ is a two-body potential à la Lennard-Jones, $\mathscr{U}_2$, which consists of a repulsive core and a narrow attractive well that can be expressed in the following dimensionless (and computationally convenient) form :

$$\mathscr{U}_2(\mathbf{r}) = A \left(\frac{a}{r^{18}} - \frac{1}{r^{16}} \right) \tag{2}$$

where r is the distance rescaled by the particle diameter d, while a and A are dimensionless parameters that control, respectively, the width and the depth of the potential well. The second contribution to $\mathscr{U}$ is a three-body term $\mathscr{U}_3$ that confers an angular rigidity to the interparticle bonds, which prevents the formation of dense clusters (Fig. 2). The idea is that once particles start to aggregate, their mechanical contacts can be more complex than the simple geometric contact between two perfect spheres represented by the attractive well $\mathscr{U}_2$ and, in particular, that there may be an energy cost associated to rotation of particles around each other in an aggregate made by more than two of them, due to inhomogeneity of their surfaces. For two particles both bonded to a third one and whose relative positions with respect to it are represented by the vectors $\mathbf{r}$ and $\mathbf{r}'$ (also rescaled by the particle diameter), $\mathscr{U}_3$ takes the following form:

$$\mathscr{U}_3(\mathbf{r}, \mathbf{r}') = B \Lambda(\mathbf{r}) \Lambda(\mathbf{r}') \exp \left[- \left(\frac{\mathbf{r} \cdot \mathbf{r}'}{r r'} - \cos\theta \right)^2 u^{-2} \right] \tag{3}$$

where B, θ, and u are dimensionless parameters. The radial modulation $\Lambda(r)$ that controls the strength of the interaction reads:

$$\Lambda(r) = r^{-10} \left[1 - (r/2)^{10} \right]^2 \mathscr{H}(2 - r) \tag{4}$$

where r is the distance rescaled by the particle diameter d. $\mathscr{H}$ denotes the Heaviside function, which ensures that $\mathscr{U}_3$ vanishes beyond the diameter of two particles. The potential energy in our model depends parametrically on the five dimensionless quantities: A, a, B, θ, and u. Tuning these parameters leads to a variety of mechanically stable porous microstructures (Colombo and Del Gado 2014a), and the values chosen in the following ($A = 6.27$, $a = 0.85$, $B = 67.27$, $\theta = 65°$ and $u = 0.3$) are such that a disordered and thin percolating network starts to self-assemble for low particle volume fractions ($\phi \lesssim 0.1$) at $\varepsilon \simeq 20 k_B T$ (see the

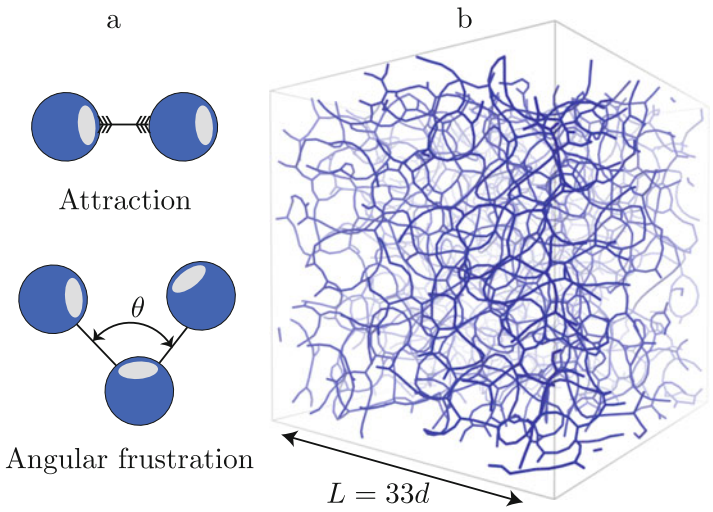

Fig. 2 (**a**) Schematic representation of the interactions: two-body attractive part and the three-body repulsive one. (**b**) Snapshot of a gel network from the simulation with number density $\rho = 0.14$, which approximately corresponds to a solid volume fraction $\phi \simeq 7.3\%$ (the sample size here is $N = 5324$ particles). Each bond is represented by a segment, when the distance d_{ij} between two particles i and j is $d_{ij} \leq 1.3d$

snapshot in Fig. 2), with k_B the Boltzmann constant and T the room temperature. Typical values of d and ε for colloidal particles range, respectively, from $d \simeq 10$ to 100 nm and from $\varepsilon \simeq 10$ to $100\, k_B T$.

With this model, we have performed molecular dynamics simulations, where the gel is composed of N particles each with a mass m in a cubic simulation box of size L. The simplicity of the model allows us to run large-scale simulations with up to $N \simeq 10^6$ particles, which is essential for a statistical analysis of the microscopic dynamics. The initial gel configuration is prepared with the protocol described in (Colombo and Del Gado 2014b), which consists in starting from a gaseous configuration at $k_B T/\varepsilon = 0.5$ and letting the gel self-assemble upon slow cooling down to $k_B T/\varepsilon = 0.05$ using Newton or Langevin equations of motion. In this temperature range, the self-assembled structures do not meaningfully depend on the specific microscopic dynamics used, and the Newtonian dynamics allows for shorter computational times. Nevertheless, once the gel has formed, the Langevin dynamics is obviously a much better choice for the dynamics overdamped by the solvent, which is typical of these materials (Colombo and Del Gado 2014a; Bouzid et al. 2017).

Once the gel is assembled, the kinetic energy is then completely drawn from the system (down to $10^{-24}\varepsilon$) by means of a dissipative microscopic dynamics:

$$m\frac{d^2\mathbf{r}_i}{dt^2} = -\nabla_{\mathbf{r}_i}\mathscr{U} - \eta_f \frac{d\mathbf{r}_i}{dt}, \tag{5}$$

where η_f is the damping coefficient associated with coupling of the particle motion to the surrounding fluid. We note that here and in the following, we always solve equations of motion that contain explicitly an inertial term with the mass m for computational convenience: integrating the equations with the inertial term allows us to use effective and precise numerical integrators (Frenkel and Smit 2002). On the other hand, the limit $m \to 0$ is the one relevant to colloidal gels in experiments, since in those systems the particle motion is completely overdamped and inertial effects are negligible. The timescales over which the particle motion is affected by inertia in our simulations are of the order of $1\tau_0 - 10\tau_0$ (for the values of m and η_f chosen). For a spherical colloidal (silica) particle of diameter $d \simeq 100\,\text{nm}$ and interaction strengths $\varepsilon \simeq 10 k_B T$, the inertial timescale $\tau_0 = \sqrt{md^2/\varepsilon} \simeq 10^{-6}\,\text{s}$ corresponds to timescales (and lengthscales, in terms of particle displacements) that are not relevant to experiments (Bouzid et al. 2018a). In the following, we make sure to be in the overdamped regime of the dynamics by choosing large enough values of η_f (Colombo and Del Gado 2014a; Puosi et al. 2014).

We also note that what is still missing in the equations of motion we discuss (here and in the following) is a proper treatment of the hydrodynamic interactions that in principle can have a strong impact on the microscopic dynamics of soft gels. While a well-established rigorous framework is still under construction, recent works indicate that the role of (long range) hydrodynamics on the emerging microscopic dynamics of the gel network at rest and in the linear response regime may be relatively negligible (Varga et al. 2015; Varga and Swan 2018; Royall et al. 2015). The main difference detected so far is a slight shift of the gelation threshold (Varga et al. 2015), which could be also due to the limited size of the numerical samples, and a tendency to favor the formation of more open and anisotropic aggregates in the early stages of the aggregation, which may significantly modify the gel formation but seems to have little consequences for the long-time relaxation dynamics in the solidified gel (Varga et al. 2015; Royall et al. 2015). The explanation for such little effect could be in the fact that once the gel is formed, the main contribution to the stresses is through the gel structure, its elasticity, and the extended soft modes present. The latter are determined by the disordered network topology and involve lengthscales of the order of the sample size. Such contributions seem to dominate the gel response with respect to the hydrodynamics coupling, which would dominate only after a significant modification/rupture/destabilization of the gel structure has taken place. Further developments for the treatment of hydrodynamic interactions in such complex materials will help elucidate this point.

In all the simulations we discuss here, the timestep δt used for the numerical integration is $\delta t = 0.005$. Distances are expressed in terms of the particle diameter d, masses in units of m, the energy in terms of the strength of the attraction ε, and the time in the units of the characteristic timescale $\tau_0 = \sqrt{md^2/\varepsilon}$. From the particle number density N/L^3, we can compute an approximate solid volume fraction $\phi \simeq N\pi d^3/6L^3$. All simulations discussed here have been performed using a version of LAMMPS suitably modified by us (Plimpton 1995).

2.2 Computing Stresses and Mechanical Response

2.2.1 Stress Calculation

The average state of stress of the gel is given by the virial stresses as $\sigma_{\alpha\beta} = -\frac{1}{L^3} \sum_i s^i_{\alpha\beta}$, where the Greek subscripts stand for the Cartesian components x, y, z, L represents the size of the system, and $s^i_{\alpha\beta}$ represents the contribution to the stress tensor of all the interactions involving the particle i (Irving and Kirkwood 1950; Thompson et al. 2009). The latter contribution is calculated for each particle, by splitting the contributions of the two-body and the three-body forces according to the following equation:

$$s^i_{\alpha\beta} = -\frac{1}{2}\sum_{n=1}^{N_2}(r^i_\alpha F^i_\beta + r'_\alpha F'_\beta) + \frac{1}{3}\sum_{n=1}^{N_3}(r^i_\alpha F^i_\beta + r'_\alpha F'_\beta + r''_\alpha F''_\beta) \tag{6}$$

The first term denotes the contribution of the two-body interaction, where the sum runs over all the N_2 pairs of interactions that involve the particle i. The couples (r^i, F^i) and (r', F') denote, respectively, the position and the forces on the two interacting particles. In the same way, the second term indicates the three-body interactions involving the particle i and two neighbors denoted by the prime and double prime quantities.

To evaluate the stress tensor at a mesoscale, we consider a coarse-graining volume v_{cg} centered around the point of interest $\mathbf{r}$ and containing around 10 particles on average and define the local coarse-grained stress based on the per-particle virial contribution as $\bar{\sigma}_{\alpha\beta}(\mathbf{r}) = -\sum_{i \in v_{cg}} s^i_{\alpha\beta}/v_{cg}$. For a typical starting configuration of the gel, the local normal stress $\bar{\sigma_n} = (\bar{\sigma}_{xx} + \bar{\sigma}_{yy} + \bar{\sigma}_{zz})/3$ reflects the heterogeneity of the structure and tends to be higher around the nodes, due to the topological frustration of the network. Note that here and in the following, we have been neglecting the kinetic contribution $-(1/L^3)\sum_i m_i \delta v^i_\alpha \delta v^i_\beta$ to the global stress tensor (from the fluctuations of the particle velocities with respect to the average), since we are mainly concerned with $\varepsilon \gg k_B T$.

2.2.2 Aging Protocol

We consider that breaking of network connections underlying the aging of the gel is more prone to happen in the regions where local stresses tend to be higher, as found also in Colombo et al. (2013) and Colombo and Del Gado (2014b). Hence aging at rest can be due to sudden ruptures of particle connections in the regions where the local tensile stresses are higher, as also suggested by experiments on ultraslow aging (Ramos and Cipelletti 2001). Such events become hardly observable on a reasonable simulation time window making it extremely challenging to study the aging regime (Colombo et al. 2013; Bouzid et al. 2017). In order to investigate the consequences of the ruptures on a timescale computationally affordable, we have devised the following dynamics: we periodically scan the local stresses in the gel structure and remove particle bonds where the local stress is the highest, with a fixed

rate Γ. In between breaking events, the gel evolution follows from the Langevin equations of motion:

$$m\frac{d^2\mathbf{r}_i}{dt^2} = -\nabla_{\mathbf{r_i}}\mathscr{U} - \eta_f\frac{d\mathbf{r}_i}{dt} + \xi_i(t), \tag{7}$$

where i refers to the particle and $\mathscr{U}$ is the interaction potential in Eq. (1). $\xi_i(t)$ is a random white noise that models the thermal fluctuations and is related to the drag coefficient η_f through its variance $\langle\xi_i(t)\xi_j(t')\rangle = 2\eta_f k_B T\delta_{ij}\delta(t-t')$. To be in the overdamped limit of the dynamics, η_f is set to 10 m/τ_0.

Recombinations of the gel branches are possible but just not observed at the volume fractions and for the time window explored here. The bonds progressively removed (by turning off the well in $\mathscr{U}_2$) are those whose contribution to the local normal stress $s_n^i = (s_{xx}^i + s_{yy}^i + s_{zz}^i)/3$ is the largest (prevalently bonds between particles belonging to the network nodes) (Bouzid et al. 2017) (see Fig. 3a). As the simulation proceeds, local internal stresses redistribute in the aging structure of the gel, and the locations of more probable connection rupture (as well as their number) change over time. All simulations presented here for the aging have been performed with a rate $\Gamma = 0.04\tau_0^{-1}$, corresponding to removing only ~5% of the total network connections over the whole simulation time window.

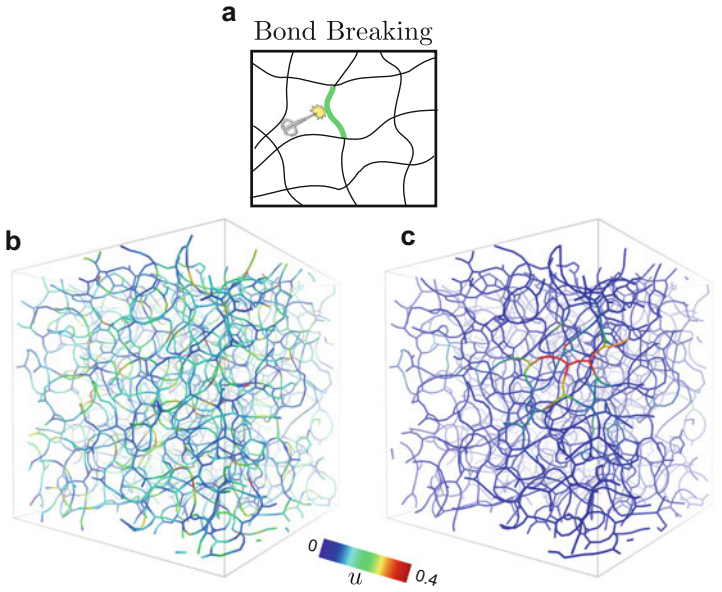

Fig. 3 (**a**) Illustration representing an irreversible elementary process in the aging simulations: breaking of a bond highlighted in green. A snapshot of the gel network is visualized using the bonds between particles, and the colors refer to the displacement field u after the bond breaking, for a network with thermal fluctuations (**b**) and for an athermal gel (**c**). (Reproduced with permission from Bouzid et al. 2017. Creative Commons license available at https://creativecommons.org/licenses/by/4.0/. Copyright 2017 Nature Publishing Group)

We have identified the range of parameters for which changing the rate (having kept all other parameters constant) does not modify the outcomes and the emerging physical picture discussed in the following. In addition to the data shown here, we have also varied the density of events, keeping fixed the criterion used for cutting (i.e., we cut the network connections corresponding to the largest tensile contributions to virial stresses). In fact, the rate of cutting events chosen for the data shown here has been chosen in a range such that the typical interval between two cutting events Γ is quite smaller than the relaxation times associated to the stress redistribution following the bond cutting. Hence many breaking events contribute to the structural relaxation that we discuss. Since for the aging we are interested to the case in which all dynamics are extremely slow (i.e., to very low temperatures in the simulations), the range of values for Γ that satisfy this condition is relatively wide. Increasing the rate corresponds to breaking a larger fraction of the total bonds initially present and hence also to increasing the density of events underlying the network rearrangements and the stress relaxation. Overall, the same results are recovered as long as the $\tau_r = 1/\Gamma$ between two rupture events allows for at least partial stress relaxation, varying Γ over nearly two orders of magnitudes. If the cutting rate is much higher, the rate may eventually disrupt the elastic strain field in the material leading to damage accumulation and spreading (Bouzid et al. 2017).

2.2.3 Start-Up Shear

To determine the gel mechanical response to a start-up shear test, each particle configuration can be submitted to a series of incremental strain steps in simple shear geometry (Colombo and Del Gado 2014b). In each step, we increase the cumulative shear strain by an amount $\delta\gamma$ by first applying an instantaneous affine deformation $\Gamma_{\delta\gamma}$, corresponding to simple shear in the xy plane, to all particles:

$$\mathbf{r}_i' = \Gamma_{\delta\gamma}\mathbf{r}_i = \begin{pmatrix} 1 & \delta\gamma & 0 \\ 0 & 1 & 0 \\ 0 & 0 & 1 \end{pmatrix} \mathbf{r}_i \tag{8}$$

The Lees-Edwards boundary conditions (Lees and Edwards 1972) are updated as well, to comply with the increase in the cumulative strain. The configuration $\{\mathbf{r}_i'\}$ is no longer a minimum of the potential energy (being the material amorphous) (Alexander 1998), and the small deformation step induces unbalanced internal forces. Hence we relax the affinely deformed configuration by letting the system free to evolve in time while keeping the global strain constant:

$$\mathbf{r}_i'' = \mathscr{T}_{\delta t}\mathbf{r}_i' \,. \tag{9}$$

where $\mathscr{T}_{\delta t}$ is the time evolution operator for a specified time interval δt and given by the damped dynamics:

$$m\frac{d^2\mathbf{r}_i}{dt^2} = -\eta_f \frac{d\mathbf{r}_i}{dt} - \nabla_{\mathbf{r}_i} U\,, \tag{10}$$

where m is the particle mass and η_f the coefficient of friction. After n steps, the cumulative strain is $\gamma_n = n\,\delta\gamma$, and the gel configuration is

$$\mathbf{r}_{i,n} = (\mathscr{T}_{\delta t}\Gamma_{\delta\gamma})^n\,\mathbf{r}_{i,0}\,, \tag{11}$$

where $\{\mathbf{r}_{i,0}\}$ denotes the configuration of the starting inherent structure.

This procedure is similar to the *athermal quasistatic* (AQS) approach extensively used to investigate the deformation behavior of amorphous solids (Tanguy et al. 2002; Maloney and Lemaître 2006; Fiocco et al. 2013), with the main difference that, instead of using an energy minimization algorithm after each affine deformation step, we follow the natural dynamics of the system (with a viscous energy dissipation) for a prescribed time interval δt. We can therefore define a finite shear rate $\dot{\gamma} = \delta\gamma/\delta t$ for the deformation we apply. Disregarding effects due to the particle inertia, the microscopic dynamics (10) introduce a natural timescale $\tau = \eta_f d^2/\varepsilon$, corresponding to the time it takes a particle subjected to a typical force ε/d to move a distance equal to its size. Indicatively, if we consider a typical aqueous solution of colloidal particles with a diameter $d \approx 100$ nm and an interaction energy $\varepsilon \approx 10 k_B T$ (Koumakis and Petekidis 2011), the characteristic time is $\tau \approx 10^{-4}$ s; in such a system, imposing a shear rate of $0.1\,\mathrm{s}^{-1}$ would correspond to a numerical shear rate of $\dot{\gamma}_s = 10^{-5}\tau^{-1}$.

2.2.4 Small Amplitude Oscillatory Rheology

To determine the gel viscoelastic properties, the particles are submitted to a continuous shear strain $\gamma(t)$ in the xy plane according to the following equation:

$$m\frac{d^2\mathbf{r}_i}{dt^2} = -\nabla_{\mathbf{r_i}}\mathscr{U} - \eta_f\left(\frac{d\mathbf{r}_i}{dt} - \dot{\gamma}(t) y_i \mathbf{e_x}\right) \tag{12}$$

In order to measure the frequency and the strain dependence of the first-harmonic storage G' and loss modulus G'', we impose an oscillatory shear strain on the system, i.e., the shear strain is modulated periodically according as $\gamma(t) = \gamma_0 \sin(\omega_i t)$, and we use Lees-Edwards boundary conditions while applying the deformation.

By monitoring the shear stress response of the material $\sigma(t)$ over time, we can extract the viscoelastic moduli. The storage and loss moduli can be computed from the stress response with the following expressions:

$$\begin{aligned} G'(\omega_i) &= \mathscr{R}e\left\{\frac{\tilde{\sigma}(\omega_i)}{\tilde{\gamma}(\omega_i)}\right\} \\ G''(\omega_i) &= \mathscr{I}m\left\{\frac{\tilde{\sigma}(\omega_i)}{\tilde{\gamma}(\omega_i)}\right\} \end{aligned} \tag{13}$$

where $\tilde{\sigma}$ and $\tilde{\gamma}$ are the Fourier transforms of the stress and strain signals, respectively (Macosko 1994). The whole viscoelastic spectrum is then reconstructed by performing a discrete series of tests at various frequencies, also known as "frequency sweep."

We note that the drag term used in Eq. (12) is chosen for computational convenience, but a more accurate (Galilean invariant) option would be to have the drag term depend on the relative velocities of particles within a certain range from a given one (Salerno et al. 2012; Vasisht et al. 2019), which requires longer computations. Nevertheless, the correction due to this inaccuracy seems to be negligible in all cases discussed here, since the stresses, and the related dynamics, are dominated by the interparticle interactions and the structure topology, and the correction due to the different drag term does not significantly modify the behaviors analyzed in the following.

3 Elastically Driven Dynamics upon Aging

After the gelation, the microscopic dynamics of gels slows down considerably. The nanometric size of their building blocks makes gels sensitive to thermal fluctuations, resulting in a rich and complex relaxation processes that are associated with spontaneous and thermally activated processes. The study of how these different dynamical processes emerge at rest and how the mechanical response depends on the microstructure is relevant to several applications, since the progressive aging that such materials undergo over time has a dramatic impact on their functionalities. In aging soft solids such as gels, the microscopic dynamics is expected to be akin to slower than exponential (or stretched exponential) dynamics in super-cooled liquids or glasses, due to its strongly cooperative nature fundamentally controlled by the structural disorder, as shown in several experimental and simulation studies (Segre et al. 2001; Manley et al. 2005; Bandyopadhyay et al. 2004; Jabbari-Farouji et al. 2007; Krall and Weitz 1998; Del Gado et al. 2004; Del Gado and Kob 2007; Fierro et al. 2008; Abete et al. 2008; Angelini et al. 2014; Chaudhuri et al. 2015). Nevertheless, over the last few years, time- and space-resolved measurements have often found evidence of dynamics faster than exponential (so-called compressed exponential dynamics), intermittency, and abrupt microstructural changes, raising the question of whether the aging dynamics in gels may be controlled, instead, by stress relaxation through elastic rebound of parts of the material, after local breakages occur in its structure (Cipelletti et al. 2000; Ramos and Cipelletti 2001; Bellour et al. 2003; Angelini et al. 2013; Mansel and Williams 2015; Ruta et al. 2014; Harden et al. 2012; Chung et al. 2006; Bouchaud 2008; Ferrero et al. 2014; Gao et al. 2015; Godec et al. 2014; Chaudhuri and Berthier 2017).

The difficulty to study the aging and characterize the slow relaxation processes in gels (both in experiments and in simulations) comes from the required timescales which are extremely long. The procedure briefly described in Sect. 2.2.2 allowed us to overcome some of the difficulties: we could scan the gel network and artificially remove the connections where tensile stresses are higher, to mimic the aging process

(Fig.3a) (Bouzid et al. 2017). Using that procedure, we could characterize the stress redistribution in the network during the aging and systematically vary the amount of thermal fluctuations to elucidate how the coupling between elasticity and thermal fluctuations may qualitatively change the microscopic dynamics. Figure 3b, c show the differences in the displacement field caused by breaking connections in the same gel network in the presence of different amounts of thermal fluctuations, whereas Fig. 4a–c display the initial stress heterogeneities, the stress redistribution, and the stress fluctuations during the aging. The microscopic picture that emerged from our study points to a major role played by the architecture of the network, its elasticity, and the stress heterogeneities built in upon solidification (Fig. 4a). The timescales governing stress relaxation, respectively, through thermal fluctuations and elastic recovery are key: when thermal fluctuations are weak with respect to enthalpic stress heterogeneities, the stress can still partially relax, after the breaking of network connections, through elastically driven fluctuations. Such fluctuations are intermittent, because of strong spatiotemporal correlations that persist well beyond the timescale of the simulations (Fig. 4b, 4c) or of the experiments. Hence in these conditions ($\varepsilon / k_B T \simeq 0$) the elasticity built into the solid structure controls the microscopic displacements, and the time correlations of density fluctuations decay faster than exponential, as reported in experiments and hypothesized by theories (Cipelletti and Ramos 2005; Bouchaud 2008). Brownian motion driven by thermal fluctuations, in fact, disrupts the spatial distribution of local stresses and their persistence in time, therefore favoring a gradual loss of correlations and a slow evolution of the material properties. The insight gained in this study helped us rationalize apparently contrasting findings and clarify that in elastic soft materials the presence of large stress heterogeneities can favor faster than exponential and intermittent microscopic dynamics. In addition to affecting the time evolution and the material properties rest, these dynamic processes interact with an imposed mechanical deformation and can therefore be decisive for the mechanical response of this class of soft solids.

4 Mechanical Response

A macroscopic constitutive law for soft gels, i.e., the theory capturing how stresses are related to deformations, velocities, and possibly density in these materials, is still fundamentally lacking. As an example, we give the constitutive law of a Hookean homogeneous elastic solid. In this case, the stress tensor takes the form:

$$\sigma_{\alpha\beta} = K\varepsilon_{\ell\ell}\delta_{\alpha\beta} + 2G\varepsilon_{\alpha\beta} \tag{14}$$

K represents the bulk modulus and G the shear modulus. ε_{ij} is the strain tensor of the material with respect to its reference state (Landau and Lifshitz 1986), while α and β indicate the Cartesian components. Following the same reasoning, when describing the flow of the materials in response to a rate of deformation

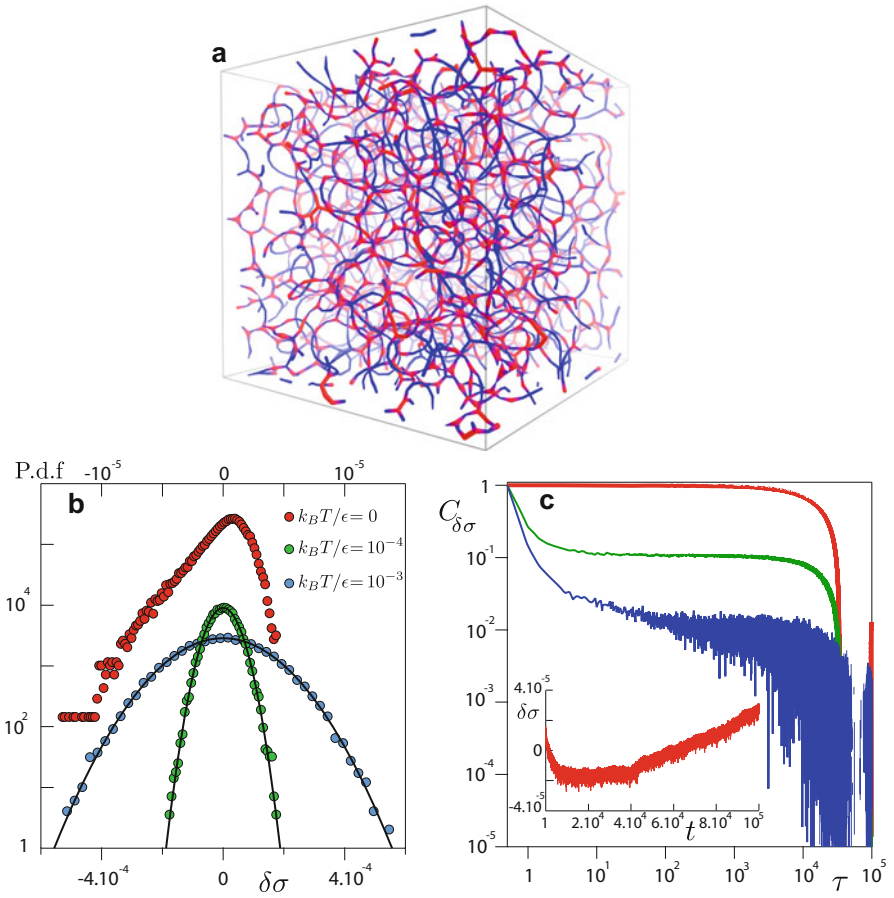

Fig. 4 (**a**) A snapshot of the initial colloidal gel network for $k_BT/\varepsilon = 0$ and at low volume fraction $\phi = 7\%$, showing the interparticle bonds represented by a segment. The colors indicate the local normal stress $\tilde{\sigma}_n$, using red for tension and blue for compression. (**b**) The corresponding P.d.f of the time series of the normal stress fluctuations $\delta\sigma = \sigma_{xx} - \langle\sigma_{xx}\rangle$: in the regime dominated by frozen-in stresses (red), the stress fluctuations are elastically driven and intermittent in nature. (**c**) Main frame: The stress fluctuation autocorrelation function measured over the whole simulation for the fully thermal regime $k_BT/\varepsilon = 10^{-3}$ (blue), the intermediate $k_BT/\varepsilon = 10^{-4}$ (green), and the for $k_BT/\varepsilon = 0$ (red). Inset: Time series of the normal stress fluctuations $\delta\sigma$ over all the simulation for the athermal sample showing the aging of the structure. (Reproduced with permission from Bouzid et al. 2017. Creative Commons license available at https://creativecommons.org/licenses/by/4.0/. Copyright 2017 Nature Publishing Group)

(e.g., due to imposed shear Fig. 7), the constitutive relation can be constructed from the strain rate tensor:

$$\dot{\gamma}_{\alpha\beta} = \frac{1}{2}\left(\frac{\partial u_\alpha}{\partial x_\beta} + \frac{\partial u_\beta}{\partial x_\alpha}\right) \tag{15}$$

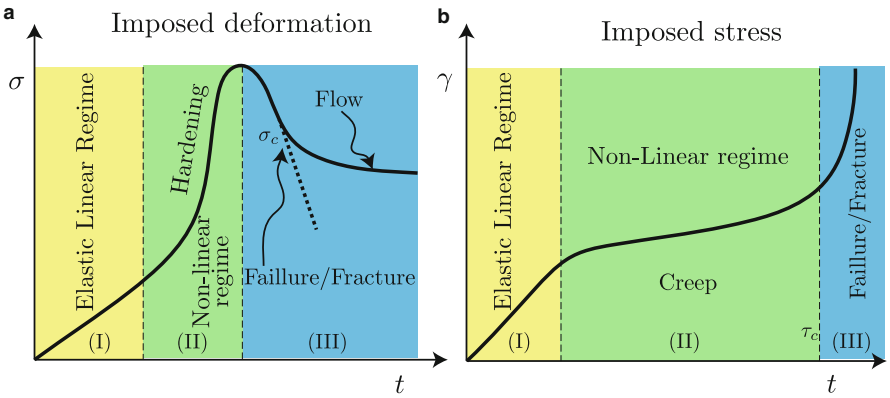

Fig. 5 Log-log scale: schematic representation of the different macroscopic responses of gels to an imposed shear deformation rate (**a**) or shear stress (**b**)

Where u_α and x_α are, respectively, the components of the velocity vector and the position along the α axis. A fluid is characterized by its viscosity η, defined as the ratio between the stress and the strain rate, and the simplest example is a Newtonian fluid, for which the stress tensor takes the form:

$$\sigma_{\alpha\beta} = (g\dot{\gamma}_{\ell\ell} - P)\delta_{\alpha\beta} + 2\eta\dot{\gamma}_{\alpha\beta} \tag{16}$$

where $\delta_{\alpha\beta}$ is the Kronecker symbol, P is the normal stress, and g is zero for an incompressible fluid. For Newtonian fluids, the viscosity is independent of the shear rate as well as the time. The only stresses created by the flow are the shear stresses that cancel out immediately when the flow stops. Any deviation from these properties is a sign of non-Newtonian behavior.

Once a gel has solidified from an initial fluid solution, its mechanical response is typically visco-elasto-plastic (Alexander 1998; Nicolas et al. 2018), with the prevalence of one behavior or the other depending on the nature of the deformation and on the observation time (Fig. 5).

4.1 Linear Response of Soft Gels

For small deformations, the response of gels is viscoelastic (regime I in Fig. 5), often exhibiting a power law frequency dependence of the elastic (G') and the viscous (G'') moduli over a wide range of frequencies (Fig. 6), reflecting a wide distribution of time and lengthscales over which the internal structures of the gel can also relax some of the residual stresses frozen-in upon solidification. These viscoelastic characteristics have been observed experimentally in a wide range of gel materials for which the porous nature of the structure can promote contraction or dilation during shear, suggesting a nontrivial coupling between the transmission of normal

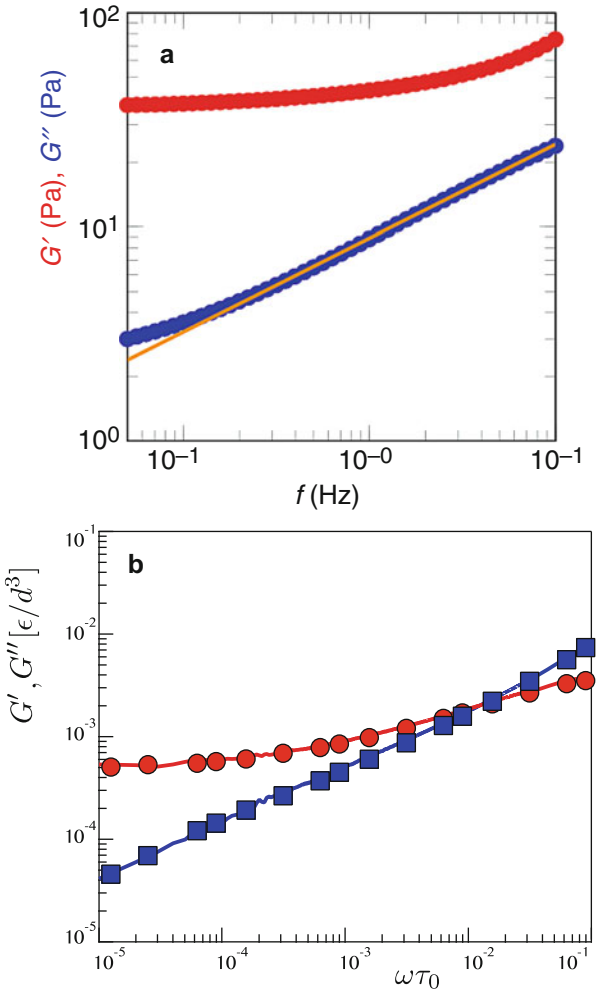

Fig. 6 (**a**) Elastic modulus G' (red) and viscous modulus G'' (blue) vs. frequency f for a carbopol gel. (Reprinted from Lidon et al. 2017). (**b**) Elastic modulus G' (squares) and viscous modulus G'' (circles) from the numerical simulations in Bouzid et al. (2018b)

and tangential forces (Ng and McKinley 2008; Caggioni et al. 2007; Jaishankar and McKinley 2014). For biopolymers networks such as collagen, G' decreases (the system becomes softer) if the system has been previously subjected to compression and increases if it is subjected to tension (Van Oosten et al. 2016). On the other hand, it has been shown that agar gels contract upon solidification (Mao et al. 2016) and that such tendency to contract is usually associated to a tendency of the material to stiffen under larger strains (Tabatabai et al. 2015; Broedersz and MacKintosh 2014; Feng et al. 2015). The changes in volume during gelation are typically coupled to

heterogeneities of internal stresses, whose consequences on the mechanical response of the material could then be controlled by adjusting the processing or preparation conditions (e.g., through the rate of confinement or gelation).

Using the model introduced in Sect. 2, recent numerical investigations have been able to reproduce these linear mechanical features (Fig. 6) and also provide a constitutive parametric model able to capture the linear response (Bouzid et al. 2018a). Classical constitutive models based on combinations of Hookean springs and dashpots, such as the Maxwell or Kelvin-Voigt model, are not able to capture the frequency dependence of the moduli (Macosko 1994). To describe these power laws, one can add different mechanical elements (Maxwell or Kelvin-Voigt) in series or in parallel, which will result in creating additional modes of relaxation of the system. This method is questionable because of the large number of elements necessary to model all the relaxation modes. A different approach is based on proposing a *fractional* model, which uses instead a spring-pot element, originally introduced by Scott Blair (Blair and Veinoglou 1944; Blair 1944) and recently applied with success to a broad variety of soft viscoelastic materials (Jaishankar and McKinley 2012; Bouzid et al. 2018a; Aime et al. 2018a).

4.2 Nonlinear Response

Upon increasing the imposed deformation, the rheological response of soft gels has strongly nonlinear characteristics, corresponding to regimes II and III in Fig. 5: soft gels can flow as yield stress fluids or fracture as solids (see examples in the cartoons of Fig. 7). The strongly nonlinear transient regimes preceding yielding or fracture are poorly understood and constitute an active area of research. In addition, the yielding or fracturing can be reversible, with the material regaining its elasticity once brought to rest, or irreversible.

Numerical simulations are a powerful tool to overcome experimental limitations and challenges, complementing them effectively. For example, imaging the structure and, at the same time, applying a deformation is not always possible, whereas simulations can be obviously more effective in connecting the structure to the

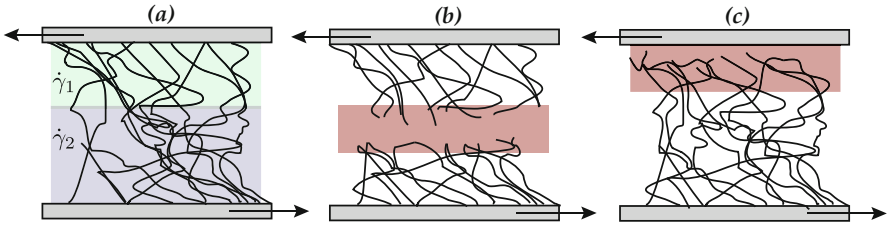

Fig. 7 Illustrations of different non-linear behaviors: (**a**) Shear band with two distinct shear rates $\dot{\gamma}_1 \neq \dot{\gamma}_2$. (**b**) Fracture in the bulk. (**c**) Loss of adhesion between the gel and the wall: sliding on the walls

mechanical response and in addressing specific microscopic mechanisms. Using the approach described in Sect. 2, for example, we have recently provided novel insight into how regimes (I–III) in Fig. 5 are sensitive to the complexity of the architecture of the network and dependent on the rate of deformation. The simulations (Fig. 8) have shown that for tightly connected networks, with smaller and more homogeneously distributed pores, the stresses can be redistributed more uniformly under the action of a mechanical load, promoting almost simultaneously rupture of many connections and favoring crack growth. Conversely, a softer and more sparsely connected network, in the same type of gel, favors the localization of the stresses and their redistribution through the abundant low frequency modes, possibly delaying microstructural damage and cracks growth to much larger deformations

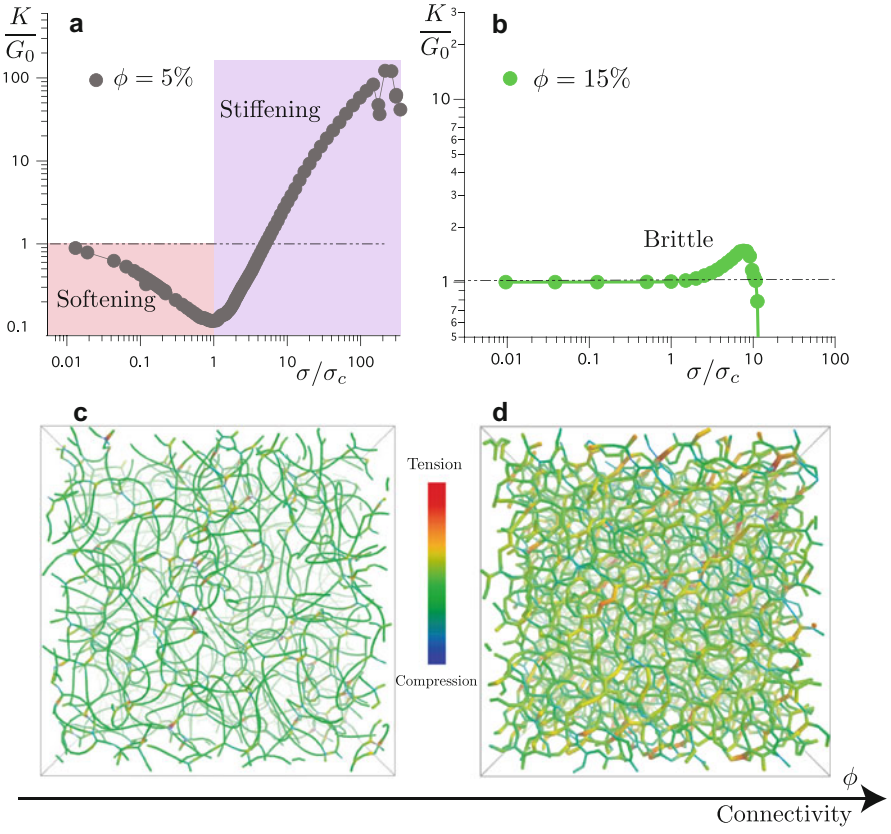

Fig. 8 The differential modulus K normalized by the elastic modulus G_0 as a function of the normalized shear stress σ/σ_c, for $\phi = 5\%$ (**a**) and $\phi = 15\%$ (**b**). Snapshots of the gel network extracted from the simulations at a volume fraction $\phi \simeq 15\%$ (**c**) and $\phi \simeq 5\%$ (**d**). Each bond is represented by a segment, when the distance d_{ij} between two particles i and j is $d_{ij} \leq 1.3d$. The color code shows the value of local tensile or compressive stresses, while the thickness is proportional to the stress amplitude. (See also Bouzid and Del Gado 2018)

(Bouzid and Del Gado 2018). Such distinct behaviors could be associated, in regime (II), to distinct dependencies of the nonlinear modulus K (obtained by deriving the shear stress σ with respect to the imposed deformation γ in the start-up shear tests described in Sect. 2) on the shear stress generated in the model materials under load (see Fig. 8). In sparse networks, extended soft modes can favor softening followed by a localization of the stresses and a progressive stiffening of the material (Figs. 8a, c). In our softer gels, the stiffening is characterized by a power law of the form $K \sim \sigma^{3/2}$, very similar the behavior of semiflexible polymer networks (Broedersz and MacKintosh 2014; Feng et al. 2016). For more homogeneously connected networks, where the gel branches are less flexible, the nonlinear response features also a progressive hardening (which is strongly rate dependent) and $K \sim \sigma$, indicating an exponential increase of the stress σ with increasing the imposed deformation γ, similar to the one observed in collagen fiber networks (Licup et al. 2015; Arevalo et al. 2015). Finally, denser networks composed of small homogeneous pores have a stronger tendency to be brittle (Fig.8b, d). It has also been shown that the ductility of the mechanical response and the reversibility of the damage accumulated under deformation can be modified by changing the flexibility of the gel branches (for a fixed network topology) and by pre-stressing the gel structures (Feng et al. 2018). Interestingly enough, in all these cases, the amount of microscopic structural anisotropy that can be induced in the gel network through deformation (and that can be quantified, for example, via a fabric tensor or a nematic order parameter suitably defined) seems a promising microscopic indicator of the nonlinear macroscopic response of different gels preceding yielding or fracture (Bouzid and Del Gado 2018; Jamali et al. 2017; Feng et al. 2015).

In the last plastic regime (III) of Fig. 5, the mechanical response depends more dramatically on the nature of the system, the specific mode of deformation (e.g., imposed stress vs deformation rate), but also on the nature of the interactions between the material and the boundaries (walls), as previously sketched in Fig. 7. Experiments show that the rupture can take place in bulk (casein-type, (bio)-polymer gels) or at the wall with a loss of adhesion and slip (agar gels, carbopol microgels, microgels of p-NIPAm, collagen, etc.) (Meeker et al. 2004; Divoux et al. 2015; Bonn et al. 2017). In spite of such complex diversity, experimental data also provide several indications that the coupling and the dynamics of localized (and correlated) plastic events may be the underlying common denominator in the transition from regime II to III. Indeed, in a variety of colloidal gels, it has been shown that in the transient regime (II) before flowing or fracturing (III), the dynamics is very intermittent in time and heterogeneous in space, featuring avalanche patterns (Kurokawa et al. 2015): in start-up shear experiments, for example, the yielding may proceed via successive drops during which the flow is spatially and temporally heterogeneous (Fig. 9a–c).

Recent experiments were able to detect a local acceleration of the microscopic dynamics before fracture and an enhancement of the plastic activity (Aime et al. 2018b). Start-up shear numerical simulations, using the approach described above, have indeed shown that the pre-yielding or pre-failure regime is dramatically rate

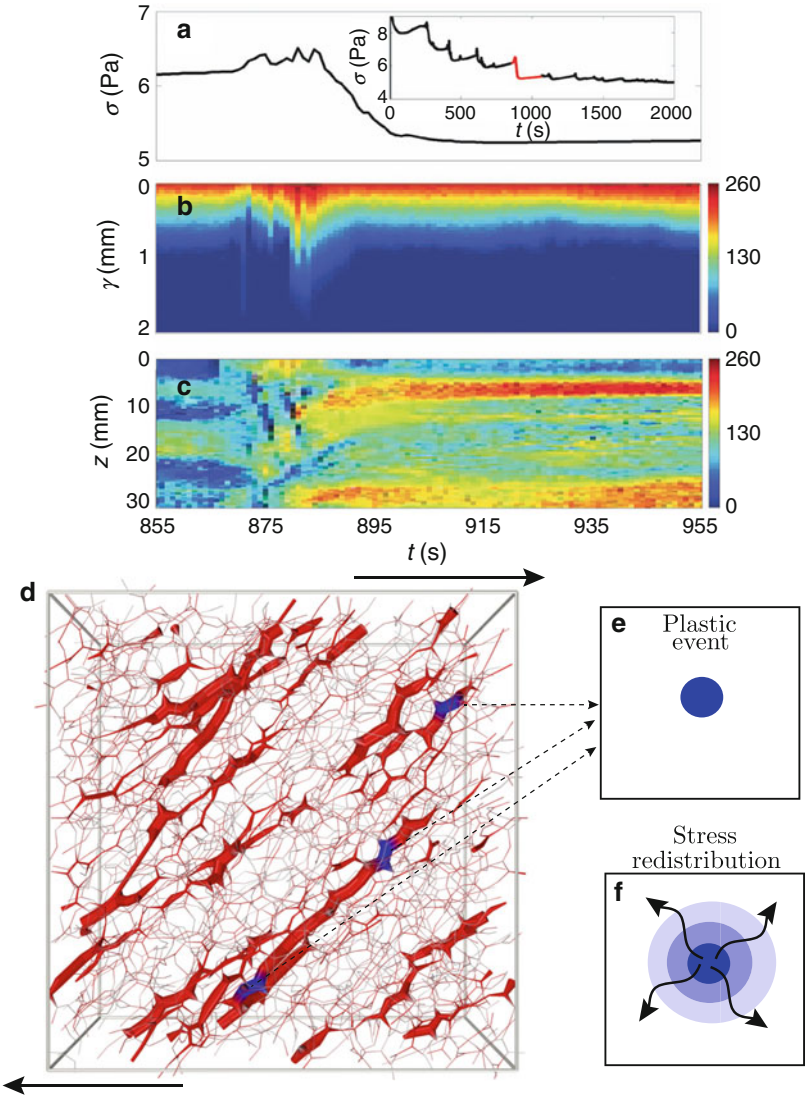

Fig. 9 Shear start-up experiment (imposed deformation) on a colloidal gel performed in a polished Taylor-Couette cell (Kurokawa et al. 2015). (**a**) The shear stress as a function of time for one stress drop (the red part of the full-time evolution shown in the inset), preceding the material fluidization. (**b**) and (**c**) are spatiotemporal intensity maps of the velocity field in the radial (**b**) and vertical (**c**) direction. (**d**) Snapshot from a numerical simulation of the model colloidal gel network discussed in Sect. 2 under shear. The thicker strands are the ones where the local tensions are larger than 60% of the maximum tensile stress. The blue indicates where breaking will happen. (Reprinted from Colombo and Del Gado 2014b). (**e**) Schematic view of the stress localization before a localized plastic event occurs inducing a nontrivial stress redistribution (**f**) across the network

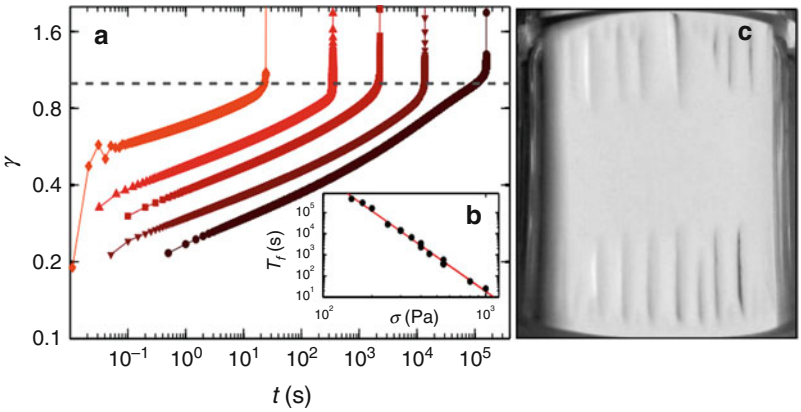

Fig. 10 Creep experiment (imposed stress σ) on a casein gels. The temporal evolution of the strain γ, for different values of shear stress σ (**a**). Three regimes are observed: an elastic regime at short time, followed by a visco-plastic regime, and finally an acceleration before rupture. (**b**) The time associated with the rupture τ_f as a function of the applied stress in a logarithmic scale, with each point corresponds to an independent creep experiment, carried out at a constant stress. The gel breaks faster when the applied stress is higher. (**c**) Snapshot of the gel before failure at $t = 0.99\tau_f$, showing regularly spaced cracks. (Reprinted from Leocmach et al. 2014)

dependent because of the coupling between the deformation rate and the dynamics of stress redistribution following localized plastic events (typically irreversible rupture of the gel connections) in a given gel network (Fig. 9d–f). Because of such coupling, the evolution at moderate or higher rate can lead to a more gradual yielding, where the dynamic correlation between the plastic events is mainly dominated by the imposed rate. Upon deforming the material at slower rate, instead, the stress redistribution dynamics in the network can itself trigger localized plastic events which are even more spatially and dynamically correlated and can enhance density fluctuations or mechanical heterogeneities in the material, eventually promoting fracture or flow instabilities (Colombo and Del Gado 2014b; Zhang et al. 2017) (Figs. 9 and 10).

In protein gels like casein, a plastic regime characterized by the clear emergence of cracks follows the initial linear viscoelastic response (Fig. 9). The resulting deformation grows as a power law over time, similar to Andrade's creep law for hard solids (Andrade 1910), and the dynamics eventually accelerates toward a catastrophic rupture (Leocmach et al. 2014, Fig. 10). The fracture time also decreases as a power law with applied stress, reminiscent of the Basquin's law of fatigue typical of hard solid as well (Basquin 1910). If the case of crystalline solids seems well understood in terms of the interaction of defects (dislocations) within the material (Csikor et al. 2007), the microscopic origin in the case of amorphous materials, and in particular for soft gels, is far from being clear, but it can be connected to the existence of localized plastic events, which act as microscopic precursors of the macroscopic failure (Aime et al. 2018b; van der Kooij et al. 2018).

5 Conclusions

Computational studies of judiciously designed models can uniquely complement new experimental approaches to provide insight into the microscopic underpinnings of the mechanical response of soft gels. Here we have given an overview and examples of recent progress in this area. The key idea is to use relatively simple but microscopic models that can include structural disorder and have complex spatiotemporal fluctuations and correlations naturally emerge from the microscopic interactions. The use of computational methods allows for solving the many-body equations of motion of interest and obtains the full spatiotemporally resolved dynamics that underlies the mechanical response of these complex materials. This comes at the cost of a few simplifications (from the very limited account of the chemical details of the specific materials to the very crude description of the solvent in which the gel matrix is embedded). We have shown that, in spite of them, one can obtain significant novel insight into the nature of the stress fluctuations acting upon aging of the material structure, into the nontrivial microstructural origin of the linear response, and into how the gel connectivity and network topology can modify dramatically the nonlinear behavior all the way to the material failure. On the one end, current challenges from the computational and theoretical side are in developing further models and approaches that can better and more efficiently capture the hydrodynamics interactions, include factors that are usually neglected but very important in experiments such as geometry and boundaries in the mechanical tests, and obtain a more quantitative understanding of the different effective interactions relevant to different material chemistry, beyond existing theories. On the other end, the results discussed here already constitute an interesting starting point to construct mesoscopic constitutive models that naturally emerge from the spatiotemporal evolution of the microstructure and its interplay with the external deformation and the deformation rate. The outstanding questions, for building such models, concern the relevant microstructural variables and the associated dynamics to be included in a continuum mechanics description of the constitutive behavior. The analysis of the spatiotemporal fluctuations, non-affine rearrangements, and local plastic events that we have briefly discussed in this chapter can help understand what are such microstructural variables and dynamics. Finally, the insight gained through studies of the type discussed here has the potential to unravel the interplay and dynamical coupling among microstructural evolution and stress redistribution in soft gels when crossing over from regime II to III in Fig. 5, providing important cues into long-standing issues such as microscopic precursors of failure, origin of creep, and hardening/toughening/self-healing mechanisms in soft materials.

Acknowledgments The authors thank the Impact Program of the Georgetown Environmental Initiative and Georgetown University for funding and the Kavli Institute for Theoretical Physics at the University of California Santa Barbara for hospitality. This research was supported in part by the National Science Foundation under Grant No. NSF PHY17-48958. EDG thanks ESPCI Paris for hospitality and support through the Chair Joliot program.

References

Abete T, de Candia A, Del Gado E, Fierro A, Coniglio A (2008) Dynamical heterogeneity in a model for permanent gels: different behavior of dynamical susceptibilities. Phys Rev E 78(4):041404

Aime S, Cipelletti L, Ramos L (2018a) Power law viscoelasticity of a fractal colloidal gel. J Rheol 62:1429–1441. https://doi.org/10.1122/1.5025622

Aime S, Ramos L, Cipelletti L (2018b) Microscopic dynamics and failure precursors of a gel under mechanical load. Proc Nat Acad Sci 115(14):3587–3592

Alexander S (1998) Amorphous solids: their structure, lattice dynamics and elasticity. Phys Rep 296(2–4):65–236

Andrade EdC (1910) Proceedings of the Royal Society of London Series A, containing papers of a mathematical and physical character, 84:1–12

Angelini R, Zulian L, Fluerasu A, Madsen A, Ruocco G, Ruzicka B (2013) Dichotomic aging behaviour in a colloidal glass. Soft Matter 9(46):10955–10959

Angelini R, Zaccarelli E, de Melo Marques FA, Sztucki M, Fluerasu A, Ruocco G, Ruzicka B (2014) Glass–glass transition during aging of a colloidal clay. Nat Commun 5:4049

Arevalo RC, Kumar P, Urbach JS, Blair DL (2015) Stress heterogeneities in sheared type-I collagen networks revealed by boundary stress microscopy. PloS one 10(3):e0118021

Bandyopadhyay R, Liang D, Yardimci H, Sessoms D, Borthwick M, Mochrie S, Harden J, Leheny R (2004) Evolution of particle-scale dynamics in an aging clay suspension. Phys Rev Lett 93(22):228302

Basquin O (1910) The Exponential Law of Endurance Tests. In: Proceedings of ASTM, vol 10, pp 625–630

Bellour M, Knaebel A, Harden J, Lequeux F, Munch JP (2003) Aging processes and scale dependence in soft glassy colloidal suspensions. Phys Rev E 67(3):031405

Bianchi E, Capone B, Kahl G, Likos CN (2015) Soft-patchy nanoparticles: modeling and self-organization. Faraday Discuss 181:123–138

Blaak R, Miller MA, Hansen JP (2007) Reversible gelation and dynamical arrest of dipolar colloids. EPL (Europhys Lett) 78(2):26002

Blair GS (1944) Analytical and integrative aspects of the stress-strain-time problem. J Sci Inst 21(5):80

Blair GS, Veinoglou B (1944) A study of the firmness of soft materials based on Nutting's equation. J Sci Inst 21(9):149

Bonn D, Denn MM, Berthier L, Divoux T, Manneville S (2017) Yield stress materials in soft condensed matter. Rev Mod Phys 89(3):035005

Boromand A, Jamali S, Maia JM (2017) Structural fingerprints of yielding mechanisms in attractive colloidal gels. Soft Matter 13(2):458–473

Bouchaud JP (2008) Anomalous relaxation in complex systems: from stretched to compressed exponentials. In: Klages R, Radons G, Sokolov IM (eds) Anomalous transport: foundations and applications. Wiley-Blackwell, pp 327–345

Bouzid M, Del Gado E (2018) Network topology in soft gels: hardening and softening materials. Langmuir 34(3):773–781

Bouzid M, Colombo J, Barbosa LV, Del Gado E (2017) Elastically driven intermittent microscopic dynamics in soft solids. Nat Commun 8:15846

Bouzid M, Keshavarz B, Geri M, Divoux T, Del Gado E, McKinley GH (2018a) Computing the linear viscoelastic properties of soft gels using an optimally windowed chirp protocol. J Rheol 62(4):1037–1050. https://doi.org/10.1122/1.5018715

Bouzid M, Keshavarz B, Geri M, Divoux T, Del Gado E, McKinley GH (2018b) Computing the linear viscoelastic properties of soft gels using an optimally windowed chirp protocol. J Rheol 62:1037. https://doi.org/10.1122/1.5018715

Broedersz CP, MacKintosh FC (2014) Modeling semiflexible polymer networks. Rev Mod Phys 86(3):995

Caggioni M, Spicer P, Blair D, Lindberg S, Weitz D (2007) Rheology and microrheology of a microstructured fluid: the gellan gum case. J Rheol 51(5):851–865
Cerbino R, Trappe V (2008) Differential dynamic microscopy: probing wave vector dependent dynamics with a microscope. Phys Rev Lett 100(18):188102
Chaudhuri P, Berthier L (2017) Ultra-long-range dynamic correlations in a microscopic model for aging gels. Phys Rev E 95(6):060601
Chaudhuri P, Hurtado PI, Berthier L, Kob W (2015) Relaxation dynamics in a transient network fluid with competing gel and glass phases. J Chem Phys 142(17):174503
Chen DT, Wen Q, Janmey PA, Crocker JC, Yodh AG (2010) Rheology of soft materials. Annu Rev Condens Matter Phys 1:301
Chung B, Ramakrishnan S, Bandyopadhyay R, Liang D, Zukoski C, Harden J, Leheny R (2006) Microscopic dynamics of recovery in sheared depletion gels. Phys Rev Lett 96(22):228301
Cipelletti L, Ramos L (2005) Slow dynamics in glassy soft matter. J Phys Condens Matter 17(6):R253
Cipelletti L, Manley S, Ball R, Weitz D (2000) Universal aging features in the restructuring of fractal colloidal gels. Phys Rev Lett 84(10):2275
Colombo J, Del Gado E (2014a) Self-assembly and cooperative dynamics of a model colloidal gel network. Soft Matter 10(22):4003–4015
Colombo J, Del Gado E (2014b) Stress localization, stiffening, and yielding in a model colloidal gel. J Rheol 58(5):1089–1116
Colombo J, Widmer-Cooper A, Del Gado E (2013) Microscopic picture of cooperative processes in restructuring gel networks. Phys Rev Lett 110(19):198301
Coniglio A, De Arcangelis L, Del Gado E, Fierro A, Sator N (2004) Percolation, gelation and dynamical behaviour in colloids. J Phys Condens Matter 16(42):S4831
Coniglio A, De Arcangelis L, De Candia A, Del Gado E, Fierro A, Sator N (2006) Clusters in attractive colloids. J Phys Condens Matter 18(36):S2383
Csikor FF, Motz C, Weygand D, Zaiser M, Zapperi S (2007) Dislocation avalanches, strain bursts, and the problem of plastic forming at the micrometer scale. Science 318(5848):251–254
De Candia A, Del Gado E, Fierro A, Sator N, Tarzia M, Coniglio A (2006) Columnar and lamellar phases in attractive colloidal systems. Phys Rev E 74(1):010403
de Cagny HC, Vos BE, Vahabi M, Kurniawan NA, Doi M, Koenderink GH, MacKintosh FC, Bonn D (2016) Porosity governs normal stresses in polymer gels. Phys Rev Lett 117(21):217802
Del Gado E, Kob W (2007) Length-scale-dependent relaxation in colloidal gels. Phys Rev Lett 98(2):028303
Del Gado E, Kob W (2010) A microscopic model for colloidal gels with directional effective interactions: network induced glassy dynamics. Soft Matter 6(7):1547–1558
Del Gado E, Fierro A, de Arcangelis L, Coniglio A (2004) Slow dynamics in gelation phenomena: from chemical gels to colloidal glasses. Phys Rev E 69(5):051103
Del Gado E, Ioannidou K, Masoero E, Baronnet A, Pellenq RM, Ulm FJ, Yip S (2014) A soft matter in construction–statistical physics approach to formation and mechanics of c–s–h gels in cement. Eur Phys J Spec Top 223(11):2285–2295
Di Michele L, Fiocco D, Varrato F, Sastry S, Eiser E, Foffi G (2014) Aggregation dynamics, structure, and mechanical properties of bigels. Soft Matter 10(20):3633–3648
Divoux T, Mao B, Snabre P (2015) Syneresis and delayed detachment in agar plates. Soft Matter 11(18):3677–3685
Duduta M, Ho B, Wood VC, Limthongkul P, Brunini VE, Carter WC, Chiang YM (2011) Semi-solid lithium rechargeable flow battery. Adv Energy Mater 1(4):511–516
Eberle AP, Porcar L (2012) Flow-sans and rheo-sans applied to soft matter. Curr Opin Colloid Interface Sci 17(1):33–43
Eberle AP, Wagner NJ, Castañeda-Priego R (2011) Dynamical arrest transition in nanoparticle dispersions with short-range interactions. Phys Rev Lett 106(10):105704
Feng D, Notbohm J, Benjamin A, He S, Wang M, Ang LH, Bantawa M, Bouzid M, Del Gado E, Krishnan R et al (2018) Disease-causing mutation in α-actinin-4 promotes podocyte detachment through maladaptation to periodic stretch. Proc Nat Acad Sci 115:1517–1522

Feng J, Levine H, Mao X, Sander LM (2015) Alignment and nonlinear elasticity in biopolymer gels. Phys Rev E 91(4):042710
Feng J, Levine H, Mao X, Sander LM (2016) Nonlinear elasticity of disordered fiber networks. Soft Matter 12(5):1419–1424
Ferrero EE, Martens K, Barrat JL (2014) Relaxation in yield stress systems through elastically interacting activated events. Phys Rev Lett 113(24):248301
Fielding SM (2014) Shear banding in soft glassy materials. Rep Prog Phys 77(10):102601
Fierro A, Del Gado E, de Candia A, Coniglio A (2008) Dynamical heterogeneities in attractive colloids. J Stat Mech Theory Exp 2008(04):L04002
Fiocco D, Foffi G, Sastry S (2013) Oscillatory athermal quasistatic deformation of a model glass. Phys Rev E 88:020301. https://doi.org/10.1103/PhysRevE.88.020301
Frenkel D, Smit B (2002) Understanding molecular simulation: from algorithms to applications, Elsevier, Amsterdam
Gallot T, Perge C, Grenard V, Fardin MA, Taberlet N, Manneville S (2013) Ultrafast ultrasonic imaging coupled to rheometry: principle and illustration. Rev Sci Inst 84(4):045107
Gao Y, Kim J, Helgeson ME (2015) Microdynamics and arrest of coarsening during spinodal decomposition in thermoreversible colloidal gels. Soft Matter 11(32):6360–6370
Godec A, Bauer M, Metzler R (2014) Collective dynamics effect transient subdiffusion of inert tracers in flexible gel networks. New J Phys 16(9):092002
Guo H, Ramakrishnan S, Harden JL, Leheny RL (2011) Gel formation and aging in weakly attractive nanocolloid suspensions at intermediate concentrations. J Chem Phys 135(15):154903
Harden J, Guo H, Ramakrishnan S, Leheny R (2012) Gel formation and aging in weakly attractive nanocolloid suspensions. In: APS meeting abstracts
Helal A, Divoux T, McKinley GH (2016) Simultaneous rheoelectric measurements of strongly conductive complex fluids. Phys Rev Appl 6(6):064004
Hsiao LC, Newman RS, Glotzer SC, Solomon MJ (2012) Role of isostaticity and load-bearing microstructure in the elasticity of yielded colloidal gels. Proc Nat Acad Sci 109(40):16029–16034
Ilg P, Del Gado E (2011) Non-linear response of dipolar colloidal gels to external fields. Soft Matter 7(1):163–171
Irving J, Kirkwood J (1950) The statistical mechanical theory of transport processes. IV. The equations of hydrodynamics. J Chem Phys 18(6):817–829
Jabbari-Farouji S, Wegdam GH, Bonn D (2007) Gels and glasses in a single system: evidence for an intricate free-energy landscape of glassy materials. Phys Rev Lett 99(6):065701
Jaishankar A, McKinley GH (2012) A fractional K-BKZ constitutive formulation for describing the nonlinear rheology of multiscale complex fluids. Power-law rheology in the bulk and at the interface: quasi-properties and fractional constitutive equations. Proc R Soc A Math Phys Eng Sci 469:20120284
Jaishankar A, McKinley GH (2014) A fractional k-bkz constitutive formulation for describing the nonlinear rheology of multiscale complex fluids. J Rheol 58(6):1751–1788
Jamali S, McKinley GH, Armstrong RC (2017) Microstructural rearrangements and their rheological implications in a model thixotropic elastoviscoplastic fluid. Phys Rev Lett 118(4):048003
Koumakis N, Petekidis G (2011) Two step yielding in attractive colloids: transition from gels to attractive glasses. Soft Matter 7(6):2456–2470
Krall A, Weitz D (1998) Internal dynamics and elasticity of fractal colloidal gels. Phys Rev Lett 80(4):778
Kurokawa A, Vidal V, Kurita K, Divoux T, Manneville S (2015) Avalanche-like fluidization of a non-Brownian particle gel. Soft Matter 11(46):9026–9037
Landau LD, Lifshitz E (1986) Theory of elasticity. Course of theoretical physics, vol 7, 3rd edn, Elsevier, Amsterdam
Landrum BJ, Russel WB, Zia RN (2016) Delayed yield in colloidal gels: creep, flow, and re-entrant solid regimes. J Rheol 60(4):783–807
Lees A, Edwards S (1972) The computer study of transport processes under extreme conditions. J Phys C Solid State Phys 5(15):1921

Leocmach M, Perge C, Divoux T, Manneville S (2014) Creep and fracture of a protein gel under stress. Phys Rev Lett 113(3):038303
Licup AJ, Münster S, Sharma A, Sheinman M, Jawerth LM, Fabry B, Weitz DA, MacKintosh FC (2015) Stress controls the mechanics of collagen networks. Proc Nat Acad Sci 112(31):9573–9578
Lidon P, Villa L, Manneville S (2017) Power-law creep and residual stresses in a carbopol gel. Rheol Acta 56(3):307–323
Lieleg O, Kayser J, Brambilla G, Cipelletti L, Bausch A (2011) Slow dynamics and internal stress relaxation in bundled cytoskeletal networks. Nat Mater 10(3):236
Lu PJ, Zaccarelli E, Ciulla F, Schofield AB, Sciortino F, Weitz DA (2008) Gelation of particles with short-range attraction. Nature 453:499
Maccarrone S, Brambilla G, Pravaz O, Duri A, Ciccotti M, Fromental JM, Pashkovski E, Lips A, Sessoms D, Trappe V et al (2010a) Ultra-long range correlations of the dynamics of jammed soft matter. Soft Matter 6(21):5514–5522
Maccarrone S, Brambilla G, Pravaz O, Duri A, Ciccotti M, Fromental JM, Pashkovski E, Lips A, Sessoms D, Trappe V, Cipelletti L (2010b) Ultra-long range correlations of the dynamics of jammed soft matter. Soft Matter 6(21):5514–5522
Macosko C (1994) Rheology. Principles, measurements, and applications. Wiley – VCH, New York
Maloney CE, Lemaître A (2006) Amorphous systems in athermal, quasistatic shear. Phys Rev E 74(1):016118
Manley S, Wyss H, Miyazaki K, Conrad J, Trappe V, Kaufman L, Reichman D, Weitz D (2005) Glasslike arrest in spinodal decomposition as a route to colloidal gelation. Phys Rev Lett 95(23):238302
Mansel BW, Williams MA (2015) Internal stress drives slow glassy dynamics and quake-like behaviour in ionotropic pectin gels. Soft Matter 11(35):7016–7023
Mao B, Divoux T, Snabre P (2016) Normal force controlled rheology applied to agar gelation. J Rheol 60(3):473–489
Mao B, Divoux T, Snabre P (2017) Impact of saccharides on the drying kinetics of agarose gels measured by in-situ interferometry. Sci Rep 7:41185
Marx D, Hutter J (2009) Ab initio molecular dynamics: basic theory and advanced methods. Cambridge University Press, Cambridge
Meeker SP, Bonnecaze RT, Cloitre M (2004) Slip and flow in pastes of soft particles: direct observation and rheology. J Rheol 48(6):1295–1320
Ng TSK, McKinley GH (2008) Power law gels at finite strains: the nonlinear rheology of gluten gels. SOR, J Rheol 52(2):417–449
Nicolas A, Ferrero EE, Martens K, Barrat JL (2018) Deformation and flow of amorphous solids: an updated review of mesoscale elastoplastic models. Rev Mod Phys 90:45006
Ohtsuka T, Royall CP, Tanaka H (2008) Local structure and dynamics in colloidal fluids and gels. EPL (Europhys Lett) 84(4):46002
Padmanabhan P, Zia R (2018) Gravitational collapse of colloidal gels: non-equilibrium phase separation driven by osmotic pressure. Soft Matter 14(17):3265–3287. https://doi.org/10.1039/c8sm00002f
Pantina JP, Furst EM (2005) Elasticity and critical bending moment of model colloidal aggregates. Phys Rev Lett 94(13):138301
Pantina JP, Furst EM (2006) Colloidal aggregate micromechanics in the presence of divalent ions. Langmuir 22(12):5282–5288
Plimpton S (1995) Fast parallel algorithms for short–range molecular dynamics. J Comput Phys 117:1–19
Puosi F, Rottler J, Barrat JL (2014) Time-dependent elastic response to a local shear transformation in amorphous solids. Phys Rev E 89(4):042302
Ramos L, Cipelletti L (2001) Ultraslow dynamics and stress relaxation in the aging of a soft glassy system. Phys Rev Lett 87(24):245503

Rovigatti L, Sciortino F (2011) Self and collective correlation functions in a gel of tetrahedral patchy particles. Mol Phys 109(23–24):2889–2896
Royall CP, Eggers J, Furukawa A, Tanaka H (2015) Probing colloidal gels at multiple length scales: the role of hydrodynamics. Phys Rev Lett 114:258302. https://doi.org/10.1103/PhysRevLett.114.258302
Ruta B, Chushkin Y, Monaco G, Cipelletti L, Pineda E, Bruna P, Giordano VM, Gonzalez-Silveira M (2012) Atomic-scale relaxation dynamics and aging in a metallic glass probed by x-ray photon correlation spectroscopy. Phys Rev Lett 109:165701
Ruta B, Czakkel O, Chushkin Y, Pignon F, Nervo R, Zontone F, Rinaudo M (2014) Silica nanoparticles as tracers of the gelation dynamics of a natural biopolymer physical gel. Soft Matter 10(25):4547–4554
Salerno KM, Maloney CE, Robbins MO (2012) Avalanches in strained amorphous solids: does inertia destroy critical behavior? Phys Rev Lett 109(10):105703
Segre P, Prasad V, Schofield A, Weitz D (2001) Glasslike kinetic arrest at the colloidal-gelation transition. Phys Rev Lett 86(26):6042
Tabatabai AP, Kaplan DL, Blair DL (2015) Rheology of reconstituted silk fibroin protein gels: the epitome of extreme mechanics. Soft Matter 11(4):756–761
Tanguy A, Wittmer J, Leonforte F, Barrat JL (2002) Continuum limit of amorphous elastic bodies: a finite-size study of low-frequency harmonic vibrations. Phys Rev B 66(17):174205
Thompson A, Plimpton S, Mattson W (2009) General formulation of pressure and stress tensor for arbitrary many-body interaction potentials under periodic boundary conditions. J Chem Phys 131:154107
Trappe V, Prasad V, Cipelletti L, Segre P, Weitz D (2001) Jamming phase diagram for attractive particles. Nature 411(6839):772
Tsurusawa H, Leocmach M, Russo J, Tanaka H (2018) Gelation as condensation frustrated by hydrodynamics and mechanical isostaticity. arXiv preprint arXiv:180404370
van Doorn JM, Verweij JE, Sprakel J, van der Gucht J (2018) Strand plasticity governs fatigue in colloidal gels. Phys Rev Lett 120(20). https://doi.org/10.1103/PhysRevLett.120.208005
Van Oosten AS, Vahabi M, Licup AJ, Sharma A, Galie PA, MacKintosh FC, Janmey PA (2016) Uncoupling shear and uniaxial elastic moduli of semiflexible biopolymer networks: compression-softening and stretch-stiffening. Sci Rep 6:19270
van der Kooij HM, Dussi S, van de Kerkhof GT, Frijns RAM, van der Gucht J, Sprakel J (2018) Laser speckle strain imaging reveals the origin of delayed fracture in a soft solid. Sci Adv 4(5). https://doi.org/10.1126/sciadv.aar1926, http://advances.sciencemag.org/content/4/5/eaar1926.full.pdf
Varga Z, Swan JW (2018) Normal modes of weak colloidal gels. Phys Rev E 97(1):012608
Varga Z, Wang G, Swan J (2015) The hydrodynamics of colloidal gelation. Soft Matter 11(46):9009–9019
Varrato F, Di Michele L, Belushkin M, Dorsaz N, Nathan SH, Eiser E, Foffi G (2012) Arrested demixing opens route to bigels. Proc Nat Acad Sci 109(47):19155–19160
Vasisht VV, Roberts G, Del Gado E (2019) Shear start-up in jammed soft solids: a computational study. arXiv:1908.03943. https://arxiv.org/abs/1908.03943
Youssry M, Madec L, Soudan P, Cerbelaud M, Guyomard D, Lestriez B (2013) Non-aqueous carbon black suspensions for lithium-based redox flow batteries: rheology and simultaneous rheo-electrical behavior. Phys Chem Chem Phys 15(34):14476–14486
Zaccarelli E, Saika-Voivod I, Buldyrev SV, Moreno AJ, Tartaglia P, Sciortino F (2006) Gel to glass transition in simulation of a valence-limited colloidal system. J Chem Phys 124(12):124908
Zhang L, Rocklin DZ, Sander LM, Mao X (2017) Fiber networks below the isostatic point: fracture without stress concentration. Phys Rev Mater 1(5):052602
Zia RN, Landrum BJ, Russel WB (2014) A micro-mechanical study of coarsening and rheology of colloidal gels: cage building, cage hopping, and Smoluchowski's ratchet. J Rheol 58(5):1121–1157